Biochemistry and Biophysics Reports 13 (2018) 78–82

Contents lists available at ScienceDirect

Biochemistry and Biophysics Reports

journal homepage: www.elsevier.com/locate/bbrep

Crystal structure analysis of human serum albumin complexed with sodium 4-phenylbutyrate

Akito Kawai[a], Keishi Yamasaki[a,b], Taisuke Enokida[a], Shuichi Miyamoto[a], Masaki Otagiri[a,b,*]

[a] Faculty of Pharmaceutical Sciences, Sojo University, 4-22-1 Ikeda, Nishi-ku, Kumamoto 860-0082, Japan
[b] DDS Research Institute, Sojo University, 4-22-1 Ikeda, Nishi-ku, Kumamoto 860-0082, Japan

ARTICLE INFO

Keywords:
Human serum albumin
X-ray crystallography
Sodium 4-phenylbutyrate
Drug interaction
Drug site 2

ABSTRACT

Sodium 4-phenylbutyrate (PB) is an orphan drug for the treatment of urea cycle disorders. It also inhibits the development of endoplasmic reticulum stress, the action of histone deacetylases and as a regulator of the hepatocanalicular transporter. PB is generally considered to have the potential for use in the treatment of the diseases such as cancer, neurodegenerative diseases and metabolic diseases. In a previous study, we reported that PB is primarily bound to human serum albumin (HSA) in plasma and its binding site is drug site 2. However, details of the binding mode of PB to HSA remain unknown. To address this issue, we examined the crystal structure of HSA with PB bound to it. The structure of the HSA–PB complex indicates that the binding mode of PB to HSA is quite similar to that for octanoate or drugs that bind to drug site 2, as opposed to that for other medium-chain length of fatty acids. These findings provide useful basic information related to drug–HSA interactions. Moreover, the information presented herein is valuable in terms of providing safe and efficient treatment and diagnosis in clinical settings.

1. Introduction

Sodium 4-phenylbutyrate (PB) is a phenyl-substituted fatty acid derivative and is clinically used for the treatment of urea cycle disorders by virtue of its ammonium scavenging activity [1,2]. Recently, in addition to its activity as a scavenger of ammonium ions, PB has also been found to be an inhibitor of endoplasmic reticulum stress and the action of histone deacetylases [3,4].

We previously reported that PB binds to a single site on HSA, identified as drug site 2, based on fluorescent probe displacement experiments. Furthermore, Tyr411 and Arg410 were identified as being involved in the binding of PB to drug site 2, based on binding experiments using chemically modified-HSAs and mutant-HSAs [5]. In addition, the same authors characterized the binding of PB to albumin from several species, including the rat [6].

In continuing our investigations, we prepared single HSA–PB complex crystals by multiple rounds of streak-seeding in an attempt to determine the three-dimensional structure of the HSA–PB complex using X-ray crystallographic analysis. The results obtained here indicate that the carboxylate group of PB is hydrogen-bonded to Arg410, Tyr411 and Ser489, and the alkyl chain, including the phenyl group of PB, occupies the hydrophobic cavity of drug site 2 surrounded by Leu387, Ile388, Asn391, Cys392, Phe403, Leu407, Arg410, Tyr411, Leu430, Gly431, Val433, Cys437, Cys438, Ala449 and Leu453. These findings provide information that will be useful for clinical applications of PB.

2. Material and methods

2.1. Crystallization of the HSA–PB complex

Preparation of the HSA solution for the crystallization was performed as described previously [7]. PB was purchased from LKT Laboratories, Inc. (St. Paul, Minnesota, USA), and the 0.1 M stock solution of PB for the crystallization was prepared by dissolving in 50 mM potassium phosphate pH 7.0. Co-crystallizations of the HSA–PB complex were performed using the hanging-drop vapor diffusion method by mixing 1.5 μL of a HSA solution (93 mg/mL HSA containing 14 mM PB) and 1.5 μL of a reservoir solution containing 28%(*w/v*) polyethylene glycol 3350, 10%(*w/v*) 2-methyl-2,4-pentandiol and 50 mM potassium phosphate pH 7.0 at 15 °C. Single HSA–PB complex crystals were obtained by multiple rounds of streak-seeding with droplets prepared by mixing 2 μL of a HSA solution (93 mg/mL HSA containing 14 mM PB) and 2 μL of the reservoir solution containing 28%(*w/v*) polyethylene glycol 3350, 10%(*w/v*) 2-methyl-2,4-pentandiol and 50 mM potassium

Abbreviations: CMPF, 3-carboxy-4-methyl-5-propyl-2-furanpropanoic acid; HAS, human serum albumin; PB, sodium 4-phenylbutyrate

* Corresponding author at: Faculty of Pharmaceutical Sciences, Sojo University, 4-22-1 Ikeda, Nishi-ku, Kumamoto 860-0082, Japan.
E-mail address: otagirim@ph.sojo-u.ac.jp (M. Otagiri).

https://doi.org/10.1016/j.bbrep.2018.01.006
Received 31 October 2017; Received in revised form 9 January 2018; Accepted 9 January 2018
Available online 28 January 2018

phosphate pH 7.0 at 15 °C and pre-equilibrated for three days.

2.2. Data-collection, structure determination and refinement

The HSA–PB complex crystals were directly frozen in liquid nitrogen. Synchrotron experiments were performed at Photon Factory BL-17A (Tsukuba, Japan). Diffraction data set was collected at −173 °C using a Pilatus3 S 6 M detector with a crystal-to-detector distance of 486 mm, an oscillation range of 0.5° per frame and an exposure time of 0.5 s per frame. A total of 720 frames were collected, and this data set was processed and scaled using *HKL2000* [8]. The initial phase of the HSA–PB complex structure was determined by the molecular replacement method using *MOLREP* [9] from the *CCP4* program suite [10], with the coordinate (PDB: 5X52 [7]) serving as the search model. Further model building was performed with *COOT* [11]. Structure refinement including the refinement of atomic displacement parameters by the translation, liberation and screw (TLS) method was performed with *phenix.refine* [12] and the TLS groups were determined by using the *phenix.find_tls_groups* from the *PHENIX* package [13]. The stereochemical quality of the final structure was evaluated by *MolProbity* [14]. All molecular graphics were prepared using *PyMOL* [15]. The atomic coordinates of the HSA–PB complex have been deposited in the Protein Data Bank under the accession code 5YOQ.

3. Results

3.1. Crystal structure of the HSA–PB complex

The HSA–PB complex crystallized in space group $P2_1$ with unit-cell parameters a = 58.5 Å, b = 181.9 Å, c = 59.5 Å and β = 105.2°, and two HSA molecules were included in the asymmetric unit. The crystal structure of the HSA–PB complex was determined at a resolution of 2.65 Å and refined to final R and R_{free} factors of 23.5% and 25.6%, respectively. Data-collection and structure refinement statistics are summarized in Table 1.

The overall structure of the HSA–PB complex forms an asymmetrical heart-shaped structure, similar to that for other previously reported HSA structures [16] (Fig. 1). The *r.m.s.d.* value between the C_α positions of each HSA–PB complex structure in the asymmetric unit is 0.63 Å for 557 aligned residues, suggesting that the two structures in the crystal are almost identical. PB is the salt of an aromatic fatty acid, therefore, we compared the HSA–PB complex structure to HSA structures complexed with the eight- to fourteen-carbons saturated fatty acids. These results show that the overall structure of the HSA–PB complex resembles the HSA–octanoate–*N*-acetyl-L-methionine complex structure (PDB: 5X52 [7], the *r.m.s.d.* value is 0.46 Å for aligned 571 residues) in comparison to the HSA structures bound to the other fatty acid, which have undergone a fatty acid binding-induced conformational change in domains I and III relative to domain II of HSA [17–20]: the *r.m.s.d.* value for the HSA–decanoic acid complex structure is 3.31 Å for 473 aligned residues (PDB: 1E7E [19]), the *r.m.s.d.* value for the HSA–dodecanoic acid structure is 3.36 Å for 476 aligned residues (PDB: 1E7F [19]) and the *r.m.s.d.* value for the HSA–myristic acid complex structure is 3.36 Å for 485 aligned residues (PDB: 1BJ5 [17]).

3.2. PB binding at drug site 2

The crystal structure of the HSA–PB complex also shows that one PB molecule is bound to drug site 2 located in sub-domain IIIA in the HSA structure (Fig. 1), and the details of the PB binding to HSA are as follows. The carboxylate group of PB is hydrogen-bonded to Arg410, Tyr411 and Ser489, and the alkyl chain, including the phenyl group of PB, occupies the hydrophobic cavity surrounded by Leu387, Ile388, Asn391, Cys392, Phe403, Leu407, Arg410, Tyr411, Leu430, Gly431, Val433, Cys437, Cys438, Ala449 and Leu453 (Fig. 2a). Structure comparisons of the HSA–PB complex with HSA structures complexed with ligands bound to drug site 2 (octanoate, ibuprofen, diflunisal, CMPF, diazepam, indoxyl sulfate, danslysarcosine, propofol and thyroxine) show that the PB binding location coincides very well with the binding locations of the ligands bound to drug site 2, except for

Table 1
Data-collection and refinement statistics.

Data-collection	
Source	Photon Factory BL−17A
wavelength (Å)	0.9800
Space group	$P2_1$
Unit-cell parameters	
length (Å)	a = 58.5, b = 181.9, c = 59.5,
angle (°)	β = 105.2
Resolution range (Å)	50.0 – 2.65 (2.70 – 2.65)
No. of observed reflections	232,151
No. of unique reflections	34,871
Multiplicity	6.7 (6.4)
Completeness (%)	99.9 (100)
R_{merge}(%)[a]	10.3 (68.8)
$\langle I/\sigma\ (I)\rangle$	35.7 (2.8)
Refinement	
Resolution (Å)	45.3 – 2.65 (2.72 – 2.65)
Reflection used	34,671 (2637)
R_{work} (%)[b]	23.5 (28.3)
R_{free} (%)[c]	25.6 (28.3)
Completeness (%)	99.9 (100)
Number of non-hydrogen atoms	8441
Protein	8407
Ligands	34
r.m.s.d. from ideality	
bond length (Å)	0.002
bond angle (°)	0.415
Average *B*-factor	86.4
Protein	86.5
Ligands	72.1
Ramachandran plot	
favored region (%)	96.0
allowed region (%)	4.0
outlier region (%)	0.0
Clashscore	3.2

Values in parentheses denote the highest resolution shell.
[a] $R_{merge} = 100 \times \Sigma_{hkl} \Sigma_i |I_i(hkl) - \langle I(hkl)\rangle| / \Sigma_{hkl} \Sigma_i I_i(hkl)$, where $\langle I(hkl)\rangle$ is the mean value of $I(hkl)$.
[b] $R_{work} = 100 \times \Sigma_{hkl} ||F_o| - |F_c|| / \Sigma_{hkl} |F_o|$, where F_o and F_c the observed and calculated structure factors, respectively. [c] R_{free} is calculated as for R_{work}, but for the test set comprising 5% reflections not used in refinement.

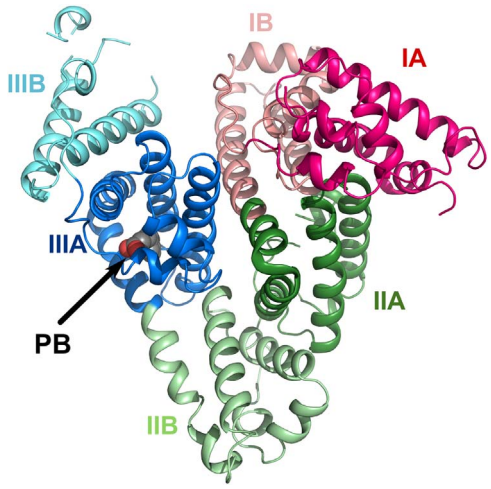

Fig. 1. Overall structure of the HSA–PB complex. The HSA molecule is shown as a cartoon representation, and the sub-domain structures are colored in magenta (IA), pink (IB), green (IIA), palegreen (IIB), blue (IIIA) and cyan (IIIB). The PB molecule (gray) is shown as a CPK representation. (For interpretation of the references to color in this figure legend, the reader is referred to the web version of this article.)

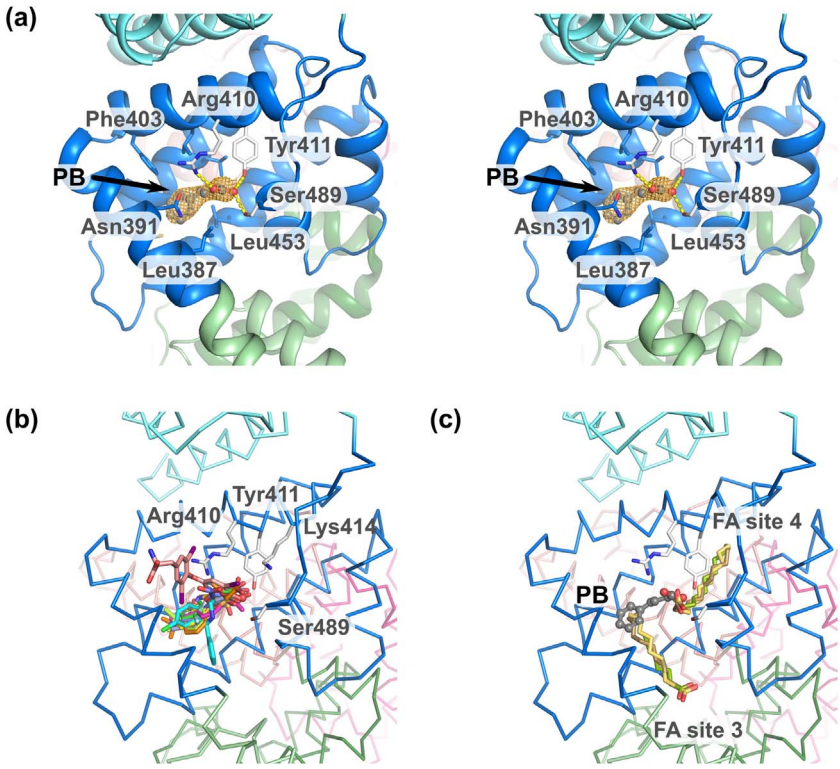

Fig. 2. PB binding at drug site 2. (a) Stereo-view of the binding of PB at drug site 2. The PB molecule (gray) is shown as a ball-and-stick representation. Hydrogen bonds are shown as yellow dashed lines. $2mF_o$-DF_c electron density maps of PB is shown as an orange mesh contoured at 1.0σ. (b) Comparisons of the binding position of PB (gray) with that of octanoate (light blue, PDB: 5X52 [7]), ibuprofen (magenta, PDB: 2BXG [28]), diflunisal (green, PDB: 2BXE [28]), CMPF (blue, PDB: 2BXA [28]), diazepam (cyan, PDB: 2BXF [28]), indoxyl sulfate (yellow, PDB: 2BXH [28]), danslysarcosine (orange, PDB: 2XVQ [34]), propofol (yellow green, PDB: 1E7A [35]) and thyroxine (pink, PDB: 1HK1 [29]). (c) Comparisons of the position of binding of PB (gray) with that of fatty acids; decanoic acid (green, PDB: 1E7E [19]), dodecanoic acid (lightorange, PDB: 1E7F [19]) and myristic acid (orange, PDB: 1BJ5 [17]). (For interpretation of the references to color in this figure legend, the reader is referred to the web version of this article.)

thyroxine (Fig. 2b). The carboxylate groups of PB, octanoate, ibuprofen, diflunisal, CMPF and danslysarcosine are hydrogen-bonded to Arg410, Tyr411, Lys414 or Ser489, that are located near the entrance to drug site 2, and the aromatic rings of PB, ibuprofen, diflunisal, danslysarcosine, diazepam, propofol and indoxyl sulfate are located in the middle of the drug site 2 cavity. The binding of PB and thyroxine to drug site 2 involve hydrogen-bonding to Tyr411 and Ser489, which both are located at the entrance to drug site 2, while the overall thyroxine molecule is oriented toward the solvent whereas the alkyl chain of PB is accommodated within the drug site 2 cavity. Fatty acids, except for octanoate, also bind to HSA near drug site 2 and these binding sites are referred to as FA sites 3 and 4 [19,21]. Structure comparisons of the HSA–PB complex to the HSA–fatty acid complex bound to FA sites 3 and 4 show that the location of the carboxylate and phenyl groups of PB coincide with the location of the carboxylate group of fatty acids bound to FA site 4 and the location of the terminal alkyl chain of the fatty acids bound to FA site 3, respectively (Fig. 2c).

4. Discussion

Information regarding the binding of endo-exogenous ligands to HSA has contributed the drug developments including the pharmacokinetics and pharmacological effects of such drugs. Very recently, in a study using specific fluorescent probes, we reported that PB binds to drug site 2. In addition, on the basis of the experimental results for the binding of PB to chemically modified HSAs (Trp modification and Tyr modification), we proposed that Tyr411, a typical residue in the drug site 2 region, is involved in PB binding. This hypothesis was supported by the binding of PB to mutant-HSAs (Y411A and R410A), for which the binding of PB to the two mutant-HSAs was decreased significantly [5,6]. It therefore appears that Arg410 as well as Tyr411 play an important role in the binding of PB to drug site 2. The crystal structure of the PB–HSA complex served to confirm the above findings. A comparison of the PB–HSA complex with HSA complexed with ibuprofen indicate that the structures are similar. This suggests that PB can be displaced by most site 2 drugs. In fact, *in vitro*, diclofenac is displaced by 6-methoxy-2-naphylacetic acid, the active metabolite of nabumetone. Moreover, the same authors found that the pain relief in rheumatoid arthritis patients using a diclofenac suppository was increased by the simultaneous oral administration of nabumetone [22]. They confirmed that the concentration of free diclofenac was increased when used in combination with nabumetone but no change in metabolism of diclofenac by CYP2C9, the rate-limiting enzyme in the metabolic clearance of diclofenac, was observed [22]. Similar observations were reported in the same laboratory when combination therapy involving the injection of flurbiprofen was applied [23]. Thus, the transient change in the free drug concentration due to displacement may influence its pharmacological activity in some cases.

Information concerning the binding sites of other types of endogenous ligands (fatty acid, sugar, heme, 4*Z*,15*E*-bilirubin-IXα, Δ^{12}-prostaglandin J2, indoxyl sulfate, CMPF and thyroxine) to HSA that were determined by X-ray crystallography are shown in Fig. 3. Fatty acid binding sites are ubiquitous in the HSA structure [19,21]. Heme, 4*Z*,15*E*-bilirubin-IXα and Δ^{12}-prostaglandin J2 bind to sub-domain IA of HSA [24–26], and glucose and fructose bind to sub-domain IIA of HSA [27]. The indoxyl sulfate and CMPF binding sites are located in both sub-domains IIA and IIIA of HSA [28], and the thyroxine binding sites are observed at sub-domains IIA, IIIA and IIIB of HSA [29]. Thus, it would be expected that PB would compete with fatty acids, indoxyl sulfate, CMPF and thyroxine for the binding to HSA, but that it would not compete with sugars, heme, 4*Z*,15*E*-bilirubin-IXα and Δ^{12}-prostaglandin J2 for binding because the location of the PB binding site is different from their binding sites in HSA. In addition, the high affinity binding sites of both long- and medium-chain length of fatty acids have been shown to be at sub-domains IIIA (FA site 4) and IIIB (FA site 5) and the primary binding site of indoxyl sulfate is located in sub-domain IIIA [28,30–32], whereas the primary binding sites of CMPF and thyroxine are located in sub-domain IIA [28,29]. Therefore, fatty acids and indoxyl sulfate would function as stronger competitive inhibitors for the binding of PB to HSA than would CMPF and thyroxine.

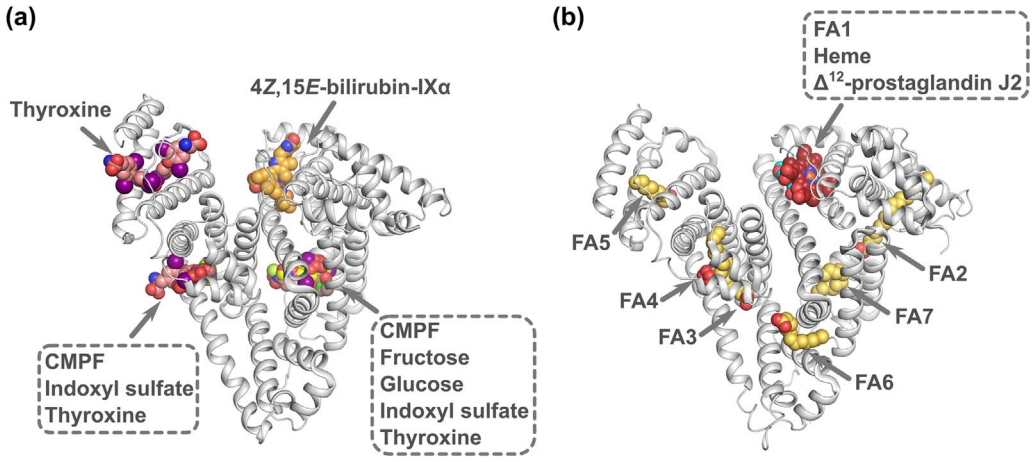

Fig. 3. The endogenous ligands binding in HSA. Ligands bound to HSA are shown as CPK representations; dodecanoic acids (lightorange, PDB: 1E7F [19]), heme (red, PDB: 1N5U [24]), Δ^{12}-prostaglandin J2 (cyan, PDB: 3A73 [26]), 4*Z*,15*E*-bilirubin-IXα (orange, PDB: 2VUE [25]), fructose (green, PDB: 4IW1 [27]), glucose (yellow green, PDB: 4IW2 [27]), CMPF (blue, PDB: 2BXA [28]), indoxyl sulfate (yellow, PDB: 2BXH [28]), and thyroxine (pink, PDB: 1HK1 [29]). Defatted (a) and fatted (b) HSA structures are shown separately because it is well known that the binding of fatty acids induces a conformational change in the molecule. Fatty acid binding sites are abbreviated as FA. (For interpretation of the references to color in this figure legend, the reader is referred to the web version of this article.)

5. Conclusion

The three-dimensional structure of the HSA–PB complex was determined in order to clarify the detailed interaction mode of PB with HSA using X-ray crystallographic analysis. Structure comparisons of the HSA–PB complex with HSA structures complexed with the site 2 drug, ibuprofen, show that the location of PB binding coincides very well with the locations where ligands are bound, as expected from the similarities of the structures of the two drugs. The carboxylate groups of PB and ibuprofen are hydrogen-bonded to Arg410, Tyr411 or Ser489, which are located near the drug site 2 entrance, and the aromatic rings of the two drugs are located in the middle of the drug site 2 cavity. An elucidation of mechanism for the molecular interaction of PB to HSA provides valuable and useful information for developing an understanding of the pharmacokinetics and the pharmacologic effects of PB in humans [33].

Acknowledgements

Synchrotron experiments were performed with the approval of the Photon Factory Program Advisory Committee (Proposal No. 2015G692, 2016R-024). This work was supported by the Platform Project for Supporting in Drug Discovery and Life Science Research (Platform for Drug Discovery, Informatics, and Structural Life Science) from the Japan Agency for Medical Research and Development (AMED). We are grateful to Professor Naohiro Matsugaki and the beamline and project staff for their support of our synchrotron experiments.

Appendix A. Supporting information

Supplementary data associated with this article can be found in the online version at http://dx.doi.org/10.1016/j.bbrep.2018.01.006.

References

[1] S.W. Brusilow, N.E. Maestri, Urea cycle disorders: diagnosis, pathophysiology, and therapy, Adv. Pediatr. 43 (1996) 127–170.
[2] T. Iannitti, B. Palmieri, Clinical and experimental applications of sodium phenylbutyrate, Drugs RD 11 (2011) 227–249, http://dx.doi.org/10.2165/11591280-000000000-00000.
[3] S. Basseri, S. Lhoták, A.M. Sharma, R.C. Austin, The chemical chaperone 4-phenylbutyrate inhibits adipogenesis by modulating the unfolded protein response, J. Lipid Res. 50 (2009) 2486–2501, http://dx.doi.org/10.1194/jlr.M900216-JLR200.
[4] A.C. Miller, S. Cohen, M. Stewart, R. Rivas, P. Lison, Radioprotection by the histone deacetylase inhibitor phenylbutyrate, Radiat. Environ. Biophys. 50 (2011) 585–596, http://dx.doi.org/10.1007/s00411-011-0384-7.
[5] T. Enokida, K. Yamasaki, Y. Okamoto, K. Taguchi, T. Ishiguro, T. Maruyama, H. Seo, M. Otagiri, Tyrosine411 and Arginine410 of human serum albumin play an important role in the binding of sodium 4-phenylbutyrate to site II, J. Pharm. Sci. 105 (2016) 1987–1994, http://dx.doi.org/10.1016/j.xphs.2016.03.012.
[6] K. Yamasaki, T. Enokida, K. Taguchi, S. Miyamura, A. Kawai, S. Miyamoto, T. Maruyama, H. Seo, M. Otagiri, Species differences in the binding of sodium 4-phenylbutyrate to serum albumin, J. Pharm. Sci. 106 (2017) 2860–2867, http://dx.doi.org/10.1016/j.xphs.2017.04.025.
[7] A. Kawai, V.T.G. Chuang, Y. Kouno, K. Yamasaki, S. Miyamoto, M. Anraku, M. Otagiri, Crystallographic analysis of the ternary complex of octanoate and N-acetyl-L-methionine with human serum albumin reveals the mode of their stabilizing interactions, Biochim. Biophys. Acta. 1865 (2017) 979–984, http://dx.doi.org/10.1016/j.bbapap.2017.04.004.
[8] Z. Otwinowski, W. Minor, Processing of X-ray diffraction data collected in oscillation mode, Methods Enzymol. (1997) 307–326, http://dx.doi.org/10.1016/S0076-6879(97)76066-X.
[9] A. Vagin, A. Teplyakov, MOLREP: an automated program for molecular replacement, J. Appl. Crystallogr. 30 (1997) 1022–1025, http://dx.doi.org/10.1107/S0021889897006766.
[10] M.D. Winn, C.C. Ballard, K.D. Cowtan, E.J. Dodson, P. Emsley, P.R. Evans, R.M. Keegan, E.B. Krissinel, A.G.W. Leslie, A. McCoy, S.J. McNicholas, G.N. Murshudov, N.S. Pannu, E.A. Potterton, H.R. Powell, R.J. Read, A. Vagin, K.S. Wilson, Overview of the CCP4 suite and current developments, Acta Crystallogr. D Biol. Crystallogr. 67 (2011) 235–242, http://dx.doi.org/10.1107/S0907444910045749.
[11] P. Emsley, B. Lohkamp, W.G. Scott, K. Cowtan, Features and development of Coot, Acta Crystallogr. D Biol. Crystallogr. 66 (2010) 486–501, http://dx.doi.org/10.1107/S0907444910007493.
[12] P.V. Afonine, R.W. Grosse-Kunstleve, N. Echols, J.J. Headd, N.W. Moriarty, M. Mustyakimov, T.C. Terwilliger, A. Urzhumtsev, P.H. Zwart, P.D. Adams, Towards automated crystallographic structure refinement with phenix.refine, Acta Crystallogr. D Biol. Crystallogr. 68 (2012) 352–367, http://dx.doi.org/10.1107/S0907444912001308.
[13] P.D. Adams, P.V. Afonine, G. Bunkóczi, V.B. Chen, I.W. Davis, N. Echols, J.J. Headd, L.W. Hung, G.J. Kapral, R.W. Grosse-Kunstleve, A.J. McCoy, N.W. Moriarty, R. Oeffner, R.J. Read, D.C. Richardson, J.S. Richardson, T.C. Terwilliger, P.H. Zwart, PHENIX: a comprehensive python-based system for macromolecular structure solution, Acta Crystallogr. D Biol. Crystallogr. 66 (2010) 213–221, http://dx.doi.org/10.1107/S0907444909052925.
[14] I.W. Davis, A. Leaver-Fay, V.B. Chen, J.N. Block, G.J. Kapral, X. Wang, L.W. Murray, W.B. Arendall, J. Snoeyink, J.S. Richardson, D.C. Richardson, MolProbity: all-atom contacts and structure validation for proteins and nucleic acids, Nucleic Acids Res. 35 (2007) W375–W383, http://dx.doi.org/10.1093/nar/gkm216.
[15] The PyMOL Molecular Graphics System, Version 1.8, Schrödinger, LLC.
[16] X.M. He, D.C. Carter, Atomic structure and chemistry of human serum albumin, Nature 358 (1992) 209–215, http://dx.doi.org/10.1038/358209a0.
[17] S. Curry, H. Mandelkow, P. Brick, N. Franks, Crystal structure of human serum albumin complexed with fatty acid reveals an asymmetric distribution of binding sites, Nat. Struct. Biol. 5 (1998) 827–835, http://dx.doi.org/10.1038/1869.
[18] S. Curry, P. Brick, N.P. Franks, Fatty acid binding to human serum albumin: new insights from crystallographic studies, Biochim. Biophys. Acta 1441 (1999) 131–140, http://dx.doi.org/10.1016/S1388-1981(99)00148-1.
[19] A.A. Bhattacharya, T. Grüne, S. Curry, Crystallographic analysis reveals common modes of binding of medium and long-chain fatty acids to human serum albumin, J. Mol. Biol. 303 (2000) 721–732, http://dx.doi.org/10.1006/jmbi.2000.4158.
[20] S. Curry, Lessons from the crystallographic analysis of small molecule binding to human serum albumin, Drug Metab. Pharmacokinet. 24 (2009) 342–357, http://dx.doi.org/10.2133/dmpk.24.342.
[21] I. Petitpas, T. Grüne, A.A. Bhattacharya, S. Curry, Crystal structures of human serum albumin complexed with monounsaturated and polyunsaturated fatty acids, J. Mol. Biol. 314 (2001) 955–960, http://dx.doi.org/10.1006/jmbi.2000.5208.
[22] N. Setoguchi, N. Takamura, K. Fujita, K. Ogata, J. Tokunaga, T. Nishio, E. Chosa, K. Arimori, K. Kawai, R. Yamamoto, A diclofenac suppository-nabumetone combination therapy for arthritic pain relief and a monitoring method for the diclofenac binding capacity of HSA site II in rheumatoid arthritis, Biopharm. Drug Dispos. 34 (2013) 125–136, http://dx.doi.org/10.1002/bdd.1829.
[23] K. Ogata, N. Takamura, J. Tokunaga, K. Kawai, K. Arimori, S. Higuchi, Dosage plan

of a flurbiprofen injection product using inhibition of protein binding by lipid emulsion in rats, J. Pharm. Pharmacol. 60 (2008) 15–20, http://dx.doi.org/10.1211/jpp.60.1.0002.
[24] M. Wardell, Z. Wang, J.X. Ho, J. Robert, F. Ruker, J. Ruble, D.C. Carter, The Atomic Structure of Human Methemalbumin at 1.9 Å, Biochem. Biophys. Res. Commun. 291 (2002) 813–819, http://dx.doi.org/10.1006/bbrc.2002.6540.
[25] P.A. Zunszain, J. Ghuman, A.F. McDonagh, S. Curry, Crystallographic analysis of human serum albumin complexed with 4Z,15E-bilirubin-IXα, J. Mol. Biol. 381 (2008) 394–406, http://dx.doi.org/10.1016/j.jmb.2008.06.016.
[26] S. Yamaguchi, G. Aldini, S. Ito, N. Morishita, T. Shibata, G. Vistoli, M. Carini, K. Uchida, Δ12-Prostaglandin J2 as a product and ligand of human serum albumin: formation of an unusual covalent adduct at His146, J. Am. Chem. Soc. 132 (2010) 824–832, http://dx.doi.org/10.1021/ja908878n.
[27] Y. Wang, H. Yu, X. Shi, Z. Luo, D. Lin, M. Huang, Structural mechanism of ring-opening reaction of glucose by human serum albumin, J. Biol. Chem. 288 (2013) 15980–15987, http://dx.doi.org/10.1074/jbc.M113.467027.
[28] J. Ghuman, P.A. Zunszain, I. Petitpas, A.A. Bhattacharya, M. Otagiri, S. Curry, Structural basis of the drug-binding specificity of human serum albumin, J. Mol. Biol. 353 (2005) 38–52, http://dx.doi.org/10.1016/j.jmb.2005.07.075.
[29] I. Petitpas, C.E. Petersen, C.-E. Ha, A.A. Bhattacharya, P.A. Zunszain, J. Ghuman, N.V. Bhagavan, S. Curry, Structural basis of albumin-thyroxine interactions and familial dysalbuminemic hyperthyroxinemia, Proc. Natl. Acad. Sci. U.S.A. 100 (2003) 6440–6445, http://dx.doi.org/10.1073/pnas.1137188100.
[30] U. Kragh-Hansen, H. Watanabe, K. Nakajou, Y. Iwao, M. Otagiri, Chain length-dependent binding of fatty acid anions to human serum albumin studied by site-directed mutagenesis, J. Mol. Biol. 363 (2006) 702–712, http://dx.doi.org/10.1016/j.jmb.2006.08.056.
[31] J.R. Simard, P.A. Zunszain, J.A. Hamilton, S. Curry, Location of high and low affinity fatty acid binding sites on human serum albumin revealed by NMR drug-competition analysis, J. Mol. Biol. 361 (2006) 336–351, http://dx.doi.org/10.1016/j.jmb.2006.06.028.
[32] J.R. Simard, P.A. Zunszain, C.-E. Ha, J.S. Yang, N.V. Bhagavan, I. Petitpas, S. Curry, J.A. Hamilton, Locating high-affinity fatty acid-binding sites on albumin by x-ray crystallography and NMR spectroscopy, Proc. Natl. Acad. Sci. U.S.A. 102 (2005) 17958–17963, http://dx.doi.org/10.1073/pnas.0506440102.
[33] K. Yamasaki, V.T.G. Chuang, T. Maruyama, M. Otagiri, Albumin-drug interaction and its clinical implication, Biochim. Biophys. Acta. 1830 (2013) 5435–5443, http://dx.doi.org/10.1016/j.bbagen.2013.05.005.
[34] A.J. Ryan, J. Ghuman, P.A. Zunszain, C.W. Chung, S. Curry, Structural basis of binding of fluorescent, site-specific dansylated amino acids to human serum albumin, J. Struct. Biol. 174 (2011) 84–91, http://dx.doi.org/10.1016/j.jsb.2010.10.004.
[35] A.A. Bhattacharya, S. Curry, N.P. Franks, Binding of the general anesthetics propofol and halothane to human serum albumin: high resolution crystal structures, J. Biol. Chem. 275 (2000) 38731–38738, http://dx.doi.org/10.1074/jbc.M005460200.